ISSN 2359-1919 (Online)
ARTIGO CIENTÍFICO

Behavior of water infiltration phenomenon in soil in an urban park

Comportamento da infiltração de água no solo em parque urbano

Artur Paiva Coutinho[1], Edilson Gomes de França[2], Alfredo Ribeiro Neto[2], Tássia dos Anjos Tenório de Melo[2], Severino Martins dos Santos Neto[2], Vitor Hugo de Oliveira Barros[1], Lucas Ravellys Pyrrho de Alcântara[2], Antonio Celso Dantas Antonino[2]

[1]Universidade Federal de Pernambuco – UFPE, Caruaru, PE, Brasil. E-mails: arthur.coutinho@yahoo.com.br, vitor_barros1@outlook.com
[2]Universidade Federal de Pernambuco – UFPE, Recife, PE, Brasil. E-mails: edigfranca@hotmail.com, ribeiront@gmail.com, melo.tassia@yahoo.com.br, martinsdsn@gmail.com, ravellyspyrrho@gmail.com, cdantonino@gmail.com

How to cite: Coutinho, A. P., França, E. G., Ribeiro Neto, A., Melo, T. A. T., Santos Neto, S. M., Barros, V. H. O., Alcântara, L. R. P., & Antonino, A. C. D. (2020). Behavior of water infiltration phenomenon in soil in an urban park. *Revista de Gestão de Água da América Latina*, *17*, e7. https://doi.org/10.21168/rega.v17e7

ABSTRACT: The objective of this work is to evaluate the infiltration capacity and to determine the hydrodynamic parameters of three surfaces (community use, children's recreation and gardens) in an urban park in Recife/PE. The Beerkan methodology was used to determine the parameters of the water retention curve and the hydraulic conductivity curve from 24 infiltration tests. Besides that, the surfaces' water balance subjected to 365 days of rainfall was simulated with the aid of the Hydrus 1D model. The garden areas presented the higher values for maximum infiltration rates (553.58 mm.h^{-1}), followed by children's recreation areas (116.70 mm.h-1) and and community use area (18.75 mm.h^{-1}). The areas' predominant textures had no direct correlation with the saturated hydraulic conductivity (Ks), presenting values between 25.38 and 306.65 mm.h $^{-1}$ for sandy loam soils (gardens); 7.67 and 542.2 mm.h^{-1} for sandy clay loam (gardens and community use); and 4.07 and 256.86 mm.h $^{-1}$ for loamy sand (recreation). The water retention capacity was lower in the gardens, with opposite behavior in the community use areas. The Hydrus' simulations resulted in higher values of runoff and evaporation in the gardens. They showed that there is no difference in the values of cumulative infiltration in the three areas.

Keywords: Beerkan Method; Hydrus 1d; Hydrodynamic Properties; Infiltration Capacity.

RESUMO: O objetivo deste trabalho é avaliar a capacidade de infiltração e determinar os parâmetros hidrodinâmicos de três superfícies (área de convivência, de recreação infantil e jardins) em um parque urbano na cidade de Recife/PE. A metodologia Beerkan foi utilizada para determinar os parâmetros da curva de retenção de água e da curva de condutividade hidráulica, a partir de 24 ensaios de infiltração; e o modelo Hydrus 1D para simular o balanço hídrico das superfícies, submetidas a 365 dias de precipitação pluviométrica. As áreas de jardins apresentaram maiores valores de taxas máximas de infiltração (553,58 mm.h^{-1}), seguidas das áreas de recreação infantil (116,70 mm.h^{-1}) e área de convivência (18,75 mm.h^{-1}). As texturas predominantes das áreas não constataram correlação direta com a condutividade hidráulica saturada (K_s), apresentando valores entre 25,38 e 306,65 mm.h^{-1} para os solos franco-arenosos (jardins); 7,67 e 542,2 mm.h^{-1} para franco-argilo-arenosos (jardins e convivência); e 4,07 e 256,86 mm.h^{-1} para areia franca (recreação). A capacidade de retenção de água foi menor nos jardins e o comportamento oposto ocorreu nas áreas de convivência. As simulações no Hydrus resultaram em valores mais elevados de lâminas escoadas e de evaporação nos jardins, e que não há diferença de valores das lâminas infiltradas acumuladas entre as três áreas.

Palavras-chave: Método Beerkan; Hydrus 1d; Propriedades Hidrodinâmicas; Capacidade de Infiltração.

INTRODUCTION

Urbanization affects the urban landscape through the insertion of impermeable surfaces in the different scales and stages of construction. The advance of impermeabilization often carried out in a disorderly way, cause changes in soil use and occupation. This results in impacts on urban areas,

Received: April 01, 2019. Revised: December 20, 2019. Accepted: June 01, 2020.

leading to a rise of local temperatures and heat islands, a decrease of vegetation areas, an increase in the runoff speed and volume, and the occurrence of floods and overflows.

Green areas such as squares, urban parks and gardens, have a landscape, recreation, and social functions. Also, these spaces help to mitigate the negative impacts of increasing impermeable areas. Therefore, urban planning must consider green spaces in its design because they will provide equilibrium and urban sustainability (Anguluri & Narayanan, 2017). In the context of Landscape Architecture, urban parks perform contemplative functions. They aim to conserve fauna and flora, providing recreation and people's interaction with nature. Besides that, they are equipment inserted in the urban network and which mainly stand out for its benefits concerning aesthetic, recreation, physical, and mental health (Ferreira, 2007; Gomes, 2014).

Urban park projects are influenced by infrastructure, cultural and socioeconomic characteristics of the place. They area designed to meet varied uses and functions (Deutscher et al., 2019). According to Sakata & Gonçalves (2019), projects developed in the past were not conceived from an environmental or ecological balance perspective, but rather to attend social enjoyment in spaces for walking, coexistence, contemplation, recreation, and sports practices. However, from the 2000s onwards, urban park projects had a sustainable character, performing ecological functions. The designs started to focus on the implementation of permeable and wooded areas, which contribute to urban drainage, maintenance of the microclimate, and reduction of heat islands.

In addition to the landscape relevance, parks can be considered urban equipment with functionalities related to other fields inserted in the infrastructure and urban quality context. Some of these are Urban Hydrology (the function of balancing processes inherent to the hydrological cycle), Environmental Comfort (improvement of microclimate and local ventilation), and Education (incentive of environmental awareness and education).

According to Anguluri & Narayanan (2017), these other functionalities are classified as ecosystem services. They are benefits provided by parks, which the population and the urban area enjoy unconsciously and, practically, without recognizing their importance, as they are variables that are difficult to measure and monitor.

Urban parks have a high vegetation cover, which is composed either by large trees or grassy and small shrubs. In the context of Hydrology, this vegetation presence is essential because it favors the evapotranspiration process (Berland et al., 2017). On the other hand, the spaces destined to social functions, reflected in areas of coexistence and children's recreation, are generally identified by exposed soil or areas composed of sandy material, enhancing the process of water infiltration into the soil. These two processes are part of the hydrological cycle, which is strongly altered in urban areas, due to the suppression of the green regions and natural soil, which is replaced by impermeable areas (Macedo et al., 2019).

Thus, parks can be considered as urban equipment with a positive hydrological function over urban basins, when designed or adapted as indispensable elements for adequate management of urban rainwater. It is important to develop studies that quantify the contributions of parks to the urban hydrological balance, mainly due to the rapid substitution of permeable/vegetation spaces by impermeable ones (Conway et al., 2011; Santos et al., 2013; Melo et al., 2014; Anguluri & Narayanan, 2017; Berland et al., 2017; Gonzalez-Sosa et al., 2017; Deutscher et al., 2019; Phillips et al., 2019).

One way to evaluate the hydrological behavior of a park is through the individual characterization of the different surfaces that compose it. This type of analysis makes it possible to presume with more details the behavior of certain phenomena, such as infiltration and runoff. Phillips et al. (2019) analyzed the potential for rainwater infiltration in urban forest areas in Baltimore (Maryland) by analyzing the unsaturated hydraulic conductivity of these surfaces.

Areas with vegetation, mainly trees, can contribute to the reduction of runoff and improve rainwater infiltration in urban areas. This can be done by the creation of channels in the soil, which facilitate infiltration through the expansion of roots (Berland et al., 2017). Thus, the specific study of each type of surface makes it possible to obtain more representative and characteristic information and data for a given area, generating results compatible with their real conditions and performance.

In parks, one can note the presence of gardens, playgrounds, and areas for family leisure, which allows picnics. These areas are composed of soils with distinguishing geotechnical and hydrodynamic properties, which sometimes have suffered anthropization processes. This fact results in soils of complex analysis (Pedron et al., 2004).

In the face of the aforementioned information, this study investigated the hydrological performance of an urban park in the city of Recife, Pernambuco. In this way, it was analyzed the

infiltration capacity and the hydrodynamic simulation of three real surfaces (community use area, children's recreation and gardens) with different uses characteristics.

METHODOLOGY

Characterization of the study area

The city of Recife, the capital of the state of Pernambuco, is classified in the Köppen model as AS climate (tropical climate with a dry summer season) and has a humid tropical climate. The rainy season is concentrated between April and July, with an average annual total precipitation of 2,250 mm/year and an average daily maximum precipitation of 110 mm/day (Alcântara et al., 2019).

The study area was the Parque da Jaqueira, which is located in the northern area of Recife, with an area of approximately 7 hectares. This park is situated close to the parallel 08°02'12" South and the meridian 34°54'17" West (Figure 1). It includes sports and landscape areas, as well as administration environments, public restrooms, and a chapel.

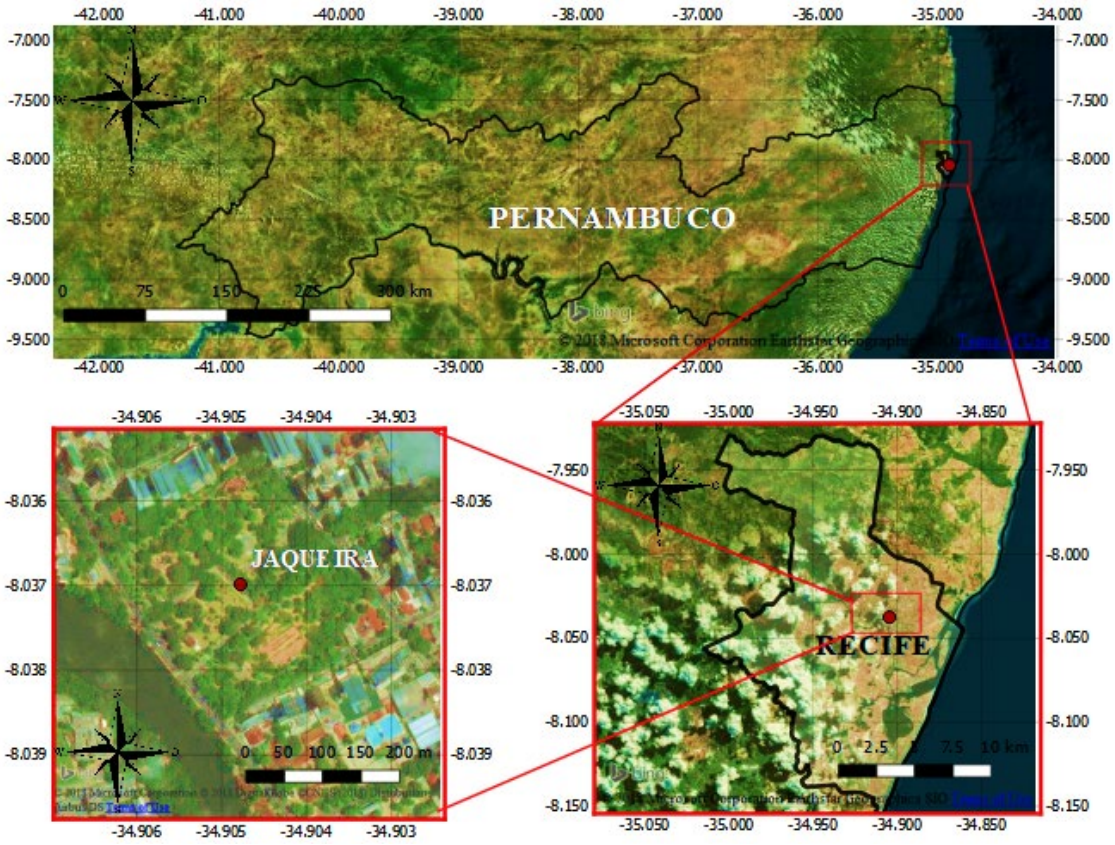

Figure 1 – Location of the study area, Parque da Jaqueira.
Source: Authors (2019).

Infiltration tests

Twente four infiltration tests were performed in 3 areas with different characteristics of coverage and soil use in order to analyze the hydrological performance of the urban park. Thus, eight experiments were performed on the soil surface of each area (Table 1).

The tests were performed with a 15 cm single ring infiltrometer, set at 1 cm deep in the soil surface as suggested by Lassabatère et al. (2006) and Angulo-Jaramillo et al. (2019). The experiments consisted of pouring defined volumes of water (70 cm^3) into the cylinder. The time interval between the insertion of one volume and another matches the time that the water layer needs to infiltrate. This process was repeated until the time between measurements became constant. This methodological process allows the determination of the infiltration capacity of the soil, resulting in curves that reflect the behavior of the cumulative infiltration as a function of time (Lassabatère et al., 2006).

Table 1 – Characterization of infiltration test sites.

Area		Use	Type of coverage	Features
Community Use	**CU**	**Community**	**Exposed soil and without any vegetation cover**	**Area with little use**
Children's Recreation	**CR**	**Leisure and recreation**	**Exposed soil and without any vegetation cover**	**Area frequently used by children**
Urban Park Gardens	**UPG**	**Contemplative**	**Grass and small shrubs**	**Area without movement of people**

Source: Authors (2019).

Before the start of each infiltration test, deformed samples were collected from the soil surface near the test point, aiming to determine the initial moisture (θ_0). After the time interval reached the steady-state, the infiltrometer was removed, and deformed soil samples were also collected from inside the ring to determine the final soil moisture (θ_f). The soil collected before the start of the experiment was also used in the determination of the particle size composition (NBR 7181 (Associação Brasileira de Normas Técnicas, 1984)).

The soil density (ρ_s) was determined from undeformed soil samples. These samples were collected using the Uhland soil sampler, and the analysis was performed in the laboratory, according to EMBRAPA (Empresa Brasileira de Pesquisa Agropecuária, 1997). Thus, for the 24 points of the infiltration tests, three soil samples were collected in the superficial layer of each area. This allowed the determination of soil grain size distribution, initial and final moisture, and density. All infiltration tests were performed on the same day, in series with approximately six infiltrometers simultaneously. The experiment with the shortest runtime was completed in around 21 minutes, and the longest lasted almost 7 hours 46 minutes.

Determination of hydraulic properties of the soil

The characterization of hydraulic properties was performed using the BEST method (Beerkan Estimation of Soil Transfer Parameters through Infiltration Experiments) (Lassabatère et al., 2006; Souza et al., 2008). This method has the advantage of providing a full characterization of the hydraulic conductivity curve and the soil water retention curve. The parameters of the hydraulic conductivity curve of the soil K (θ) were described by the model of Brooks & Corey (1964) (Equation 1). The parameters of the water retention curve h (θ) were described by the van Genuchten (1980) model with Burdine (1953) (Equation 2).

$$\frac{\mathbf{K(\theta)}}{\mathbf{K_s}} = \left(\frac{\boldsymbol{\theta} - \boldsymbol{\theta}_r}{\boldsymbol{\theta}_s - \boldsymbol{\theta}_r}\right)^{\boldsymbol{\eta}}, \mathbf{where}\ \boldsymbol{\eta} = \frac{2}{\mathbf{m}\cdot\mathbf{n}} + 2 + \mathbf{p} \tag{1}$$

$$\frac{\boldsymbol{\theta} - \boldsymbol{\theta}_r}{\boldsymbol{\theta}_s - \boldsymbol{\theta}_r} = \left[1 + \left(\frac{\mathbf{h}}{\mathbf{h_g}}\right)^{\mathbf{n}}\right]^{-\mathbf{m}}, \mathbf{where}\ \mathbf{m} = 1 - \frac{\mathbf{k_m}}{\mathbf{n}} \tag{2}$$

where θ is the volumetric moisture [$L^3 \cdot L^{-3}$]; θ_r and θ_s are the residual and saturated volumetric moisture [$L^3 \cdot L^{-3}$], respectively; h is the matrix potential [L]; h_g [L] is the scale value of h considered the potential for air intake; m and n are shape parameters; K_s is the saturated hydraulic conductivity of the soil [$L\ T^{-1}$], and η is the shape parameter for the hydraulic conductivity curve.

The BEST method requires two sets of data to estimate all hydraulic parameters: (i) the particle size distribution and the apparent density of the soil and (ii) the cumulative infiltration during the infiltration experiment and the initial and final moisture. In the BEST, θ_r is considered zero and the saturation moisture θ_s derived from the soil apparent density value, which is assumed to be equal to the porosity. The shape parameter n was estimated from a pedotransfer function developed from the particle size distribution of fractions smaller than 2 mm (Lassabatère et al., 2006). The scale parameters K_s and h_g derived from the analysis of cumulative infiltration.

The shape parameters are associated with the texture and have a similar shape between the particle size distribution F (D) and θ (h). Haverkamp & Parlange (1986) presented Equation 3 to express F (D).

$$\mathbf{F(D)}=\left[1+\left(\frac{\mathbf{D_g}}{\mathbf{D}}\right)^{\mathbf{N}}\right]^{-\mathbf{M}} \quad \text{with} \quad \mathbf{M}=1-\frac{2}{\mathbf{N}} \tag{3}$$

where D is the particle diameter [mm]; D_g is the particle size scale parameter [mm]; M and N are shape parameters of the particle size distribution curve [dimensionless].

In turn, the normalization parameters depend on the soil structure. The parameters (h_g, K_s) are obtained by minimizing I(S, K_s), that is, the squares of the differences between the observed and calculated infiltrated water layers. The infiltrated water depth is calculated using the equation proposed by Haverkamp et al. (1994), valid for short and medium periods (Equation 4).

$$\mathbf{I(S,K_s)}=\sum_{\mathbf{i=1}}^{\mathbf{Nobs}}\left(\mathbf{I_i}-\left(\mathbf{S}.\sqrt{\mathbf{t_i}}+\mathbf{a}.\mathbf{S}^2.\mathbf{t_i}+\mathbf{b}_2.\mathbf{K_s}.\mathbf{t_i}\right)\right)^2 \tag{4}$$

with:

$$\mathbf{a}=\frac{\boldsymbol{\gamma}}{\mathbf{r}.\boldsymbol{\Delta\theta}}$$

$$\mathbf{b}_2=\left(\frac{\boldsymbol{\theta}_0}{\boldsymbol{\theta}_\mathbf{s}}\right)^{\boldsymbol{\eta}}+\frac{2-\boldsymbol{\beta}}{3}.\left(1-\left(\frac{\boldsymbol{\theta}_0}{\boldsymbol{\theta}_\mathbf{s}}\right)^{\boldsymbol{\eta}}\right)$$

where S is the sorptivity; r is the radius of the cylinder; γ is equal to 0.75, and β is equal to 0.6.

To minimize the $\mathbf{I(S, K_s)}$ the Levenberg-Marquardt algorithm is used, which is an iteration technique applied to locate the minimum of a function. It is expressed as the sum of the squares of non-linear functions (Marquardt, 1963). In summary, the Levenberg-Marquardt method is simply about determining the vertex of a parabola. The performance of the adjustments is analyzed by the values that correspond to the mean square error. After obtaining the values of θ_s and K_s, the scale parameter for water pressure h_g is determined by Equation 5 (Lassabatère et al., 2006).

$$h_g=\frac{S^2}{c_p\left(\theta_s-\theta_0\right)\left[1-\left(\frac{\theta_0}{\theta_S}\right)^{\eta}\right]k_s} \tag{5}$$

where c_p is a parameter that depends only on the shape parameters n, m and η (Condappa et al., 2002; Haverkamp et al., 1998), Equation 6.

$$c_p=\Gamma\left(1+\frac{1}{n}\right)\left[\Gamma\frac{(m\eta-\frac{1}{n}}{\Gamma(m\eta)}+\frac{\Gamma\left(m\eta+m-\frac{1}{n}\right)}{\Gamma(m\eta+m)}\right] \tag{6}$$

where Γ is the classic Gamma function, which is an extension of the factorial function to the numbers.

According to Rawls et al. (1993), with the determination of hydraulic properties, one can use the saturated hydraulic conductivity (K_s) to carry out the hydrological classification of the soil. This classification divides soils into four groups: A – K_s >7.6 mm.h^{-1}; B –3.8 < K_s < 7.6 mm.h^{-1}; C – 1.3 < K_s < 1.8 mm.h^{-1}; and D – K_s < 1.3 mm.h^{-1}.

Hydrus 1D

The Hydrus-1D simulates the soil water dynamics and solute transport in porous media with different saturation levels. It solves Richards' equation (Richards, 1931) using finite elements in the spatial discretization (Equation 7), finite differences in the temporal discretization (Šimůnek et al., 2008).

$$\frac{\partial\boldsymbol{\theta}}{\partial\mathbf{t}}=\frac{\partial}{\partial\mathbf{z}}\left[\mathbf{K}\left(\frac{\partial\mathbf{h}}{\partial\mathbf{z}}+1\right)\right]-\mathbf{S} \tag{7}$$

where θ is the volumetric soil moisture [L^{-3}. L^{-3}], t is the time [T], z is the vertical coordinate [L], K (h) is the hydraulic conductivity [$L.T^{-1}$], h is the matric potential [L], and S is the root water extraction term [$L^{3}.L^{-3}.T^{-1}$]. Figure 2 shows the strategies adopted to simulate water dynamics in the study areas.

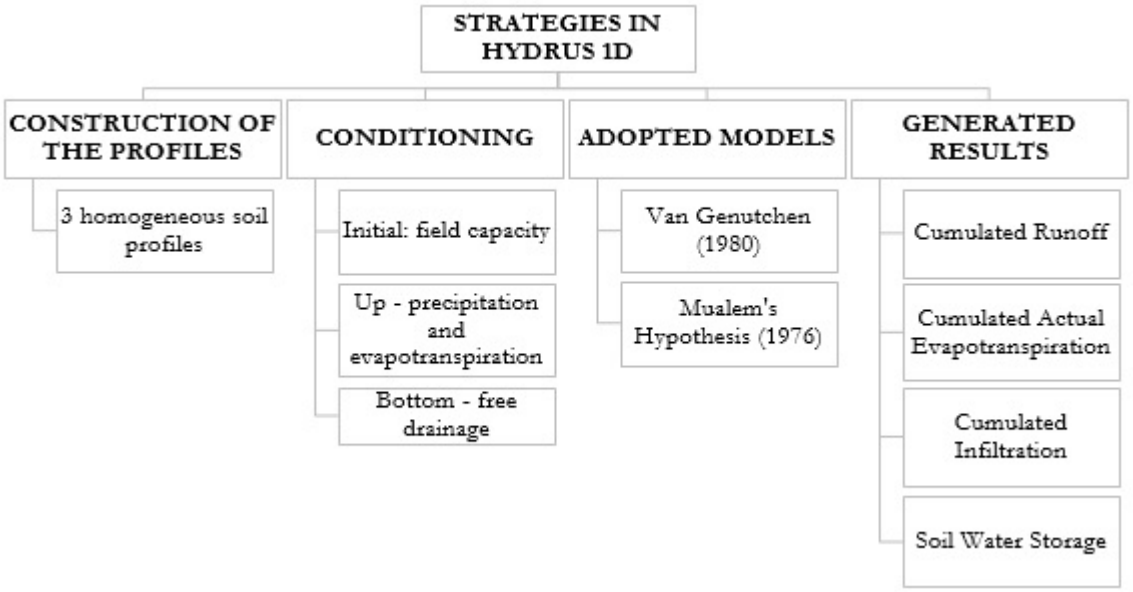

Figure 2 – Strategies adopted in the simulation of soil water transfer in Hydrus 1D.
Source: Authors (2019).

One used the Soil Profile-Graphical Editor tool to create the soil profiles, which was composed of a mesh with 600 nodes and a depth of 1 m. The hydraulic properties of each profile were recorded at the average values determined by the BEST.

Infiltration tests determined the initial soil moisture condition. For atmospheric conditions was adopted a rainfall and evapotranspiration reference series, typical for the city of Recife, with 365 days of duration, which was provided by the Agência Pernambucana de Águas e Clima (Water and Climate Agency of the Pernambuco state) for the year 2014. In the lower boundary conditions, the water table was not considered in the simulations. Thus, it was adopted free drainage of the infiltrated water.

For all cases, the model implemented to describe the hydraulic properties of the soil was that of van Genuchten (1980). Thus, as the Beerkan methodology determines the hydrodynamic parameters using Burdine's hypothesis (1953), it was necessary to adjust the pore distribution model from Burdine to Mualem (Mualem, 1976).

RESULTS AND DISCUSSIONS

Figure 3 shows the results of the infiltration experiments, referring to the cumulative infiltrated for the gathering, gathering, children's recreation and gardens areas of the urban park.

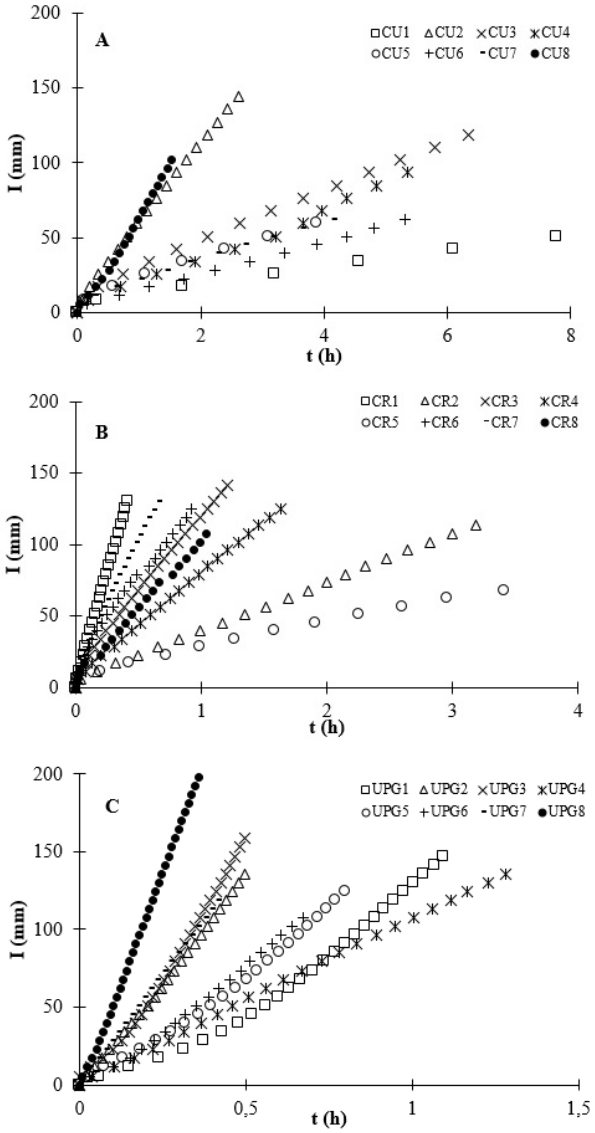

Figure 3 – Cumulative Infiltration curves for CU (A); CR (B); UPG (C).
Source: Authors (2019).

The areas destined to social interaction (A) presented lower values for the cumulative infiltration in function of time than those of areas B and C. The community use area showed maximum cumulative infiltration of 118.84 mm in 22,815 s, and the minimum was 50.93 mm in 27,980 s. These values correspond to the average infiltration rates of 18.75 and 6.55 $mm.h^{-1}$, respectively. Melo et al. (2014) also observed in a sandy clay loam soil in the city of Recife, with a similar surface as that of the social interaction area (A), and infiltration of 130.15 mm in 11,800 s. The maximum and minimum infiltration rates in the mentioned study were 327.50 $mm.h^{-1}$ and 37.94 $mm.h^{-1}$, respectively.

The children's recreation area (B) presented intermediate values in comparison to the other studied regions. The maximum cumulative infiltration was 141.47 mm in 4,364 s (116.70 $mm.h^{-1}$), while the minimum was 67.90 mm in 12,275 s (19.91 $mm.h^{-1}$). In soils of medium texture (sandy loam, loam, and sandy clay loam) and sandy (loamy sand and sand), Furtunato et al. (2013) determined infiltrations with durations between 200 and 4000 s with the infiltrated volume varying between 40 and 180 mm. In the city of Valencia (Spain), Cerdà et al. (2016) determined average infiltration rates of 10.23 and 21.65 $mm.h^{-1}$ using a rain simulator.

On the other hand, the areas with vegetated cover (C) obtained the highest values of cumulative infiltration, with a maximum of 198.06 mm in 1,288 s (553.58 $mm.h^{-1}$) and a minimum of 113.18 mm in 11,463 s (35.54 $mm.h^{-1}$). In a surface cover similar to the aforementioned, Millward et al. (2011) found, in a forest park in the city of Toronto (Canada), an average infiltration rate of 470 $mm.h^{-1}$.

The cumulative infiltration curves for C showed a steeper slope in its final part, which characterizes a higher infiltration speed, even for duration times at the end of the test. This aspect can be understood by the vegetation influence in the infiltration process, whichh allows water retantion by the plants during the tests. Besides that, the roots could also be responsible for the creation of preferential paths in the soil, which enhances a higher water flow in the soil.

The lowest infiltration values in A can be understood due to the typology of its use. Areas destined for social interaction are more subject to anthropic interventions. One of these interferences is trampling, which results in the compaction of the soil surface over time, decreasing the porosity and permeability values.

The behavior of the curves might reflect possible compaction of the soil in the community use area. From the eight tests carried out, six curves showed a performance close to the horizontality. This outcome reveals that the tests required longer times so that the same volumes of water could infiltrate.

Both the community use area and the children's recreation area have a frequent circulation of people. This configures a tendency of surface compaction, even though in the recreation area, the main flow is of infants. Thus, the relation of the curves of these zones shows that the textural difference may justify the different behavior and infiltration times in these areas. The loamy sand textural classification of the of the children's recreation area in seven analyzed points indicates a more significant presence of sand in the soil. This result provides more significant infiltration in these regions than in the sandy clay loam soil of the seven analyzed points of the community use area (Table 2).

Comparisson between the curves of community use and urban park gardens might lead to the hypothesis that the type of surface use interferes with the soil hydrological behavior. This happens even when the soils present practically the same textural classification. In this case, the presence of vegetation can potentiate the soil water infiltration through the presence of roots from the vegetation cover of the gardens (Berland et al., 2017; Phillips et al., 2019).

Regarding the grain size composition and textural classification of the 24 analyzed samples, it was found that 45% of the soils are classified as sandy clay loam, 33% as loamy sand, and 21% as sandy loam (Table 2).

Table 2 – Granulometric fractions, specific mass, and textural classification of surface soils in the CU, CR, and UPG.

Area		Sand (%)	Silt (%)	Clay (%)	Density (g/cm³)	Textural classification
Community Use (CU)	1	**85.88**	**12.33**	**1.79**	**1.59**	**Loamy Sand**
	2	**71.07**	**24.28**	**4.65**	**1.60**	**Sandy Clay Loam**
	3	**70.18**	**24.11**	**5.72**	**1.34**	**Sandy Clay Loam**
	4	**67.12**	**25.45**	**7.43**	**1.57**	**Sandy Clay Loam**
	5	**67.68**	**29.58**	**2.74**	**1.63**	**Sandy Clay Loam**
	6	**78.19**	**20.01**	**1.79**	**1.58**	**Sandy Clay Loam**
	7	**75.42**	**20.50**	**4.08**	**1.67**	**Sandy Clay Loam**
	8	**70.86**	**21.59**	**7.54**	**1.29**	**Sandy Clay Loam**
Children's Recreation (CR)	1	**85.44**	**11.58**	**2.98**	**1.54**	**Loamy Sand**
	2	**76.07**	**15.16**	**8.77**	**1.58**	**Sandy Loam**
	3	**86.80**	**13.18**	**0.02**	**1.66**	**Loamy Sand**
	4	**86.18**	**11.40**	**2.41**	**1.69**	**Loamy Sand**
	5	**85.36**	**14.08**	**0.57**	**1.54**	**Loamy Sand**
	6	**88.65**	**11.28**	**0.07**	**1.58**	**Loamy Sand**
	7	**87.08**	**11.07**	**1.85**	**1.66**	**Loamy Sand**
	8	**84.70**	**13.51**	**1.79**	**1.69**	**Loamy Sand**
Urban Park Gardens (UPG)	1	**74.44**	**23.76**	**1.79**	**1.22**	**Sandy Clay Loam**
	2	**79.48**	**17.04**	**3.48**	**1.22**	**Sandy Loam**
	3	**79.82**	**17.50**	**2.68**	**1.22**	**Sandy Loam**
	4	**75.03**	**21.54**	**3.43**	**1.38**	**Sandy Clay Loam**
	5	**78.31**	**18.95**	**2.74**	**1.25**	**Sandy Loam**
	6	**72.05**	**22.23**	**5.72**	**1.41**	**Sandy Clay Loam**
	7	**79.67**	**16.74**	**3.59**	**1.42**	**Sandy Loam**
	8	**70.26**	**25.19**	**4.55**	**1.35**	**Sandy Clay Loam**

Source: Authors (2019).

All classifications have high levels of sand in their grain size composition. The loamy characteristics of the soils, mainly the sandy clay loam, reflect in a lesser sand fraction than the loamy sand soil. However, the levels of fine particles are higher, mainly of silt material. These fractions correspond to more than 20% of the granulometric composition of the samples.

Table 3 shows the shape parameters (n, m, η), C_p, sorptivity (S), saturated hydraulic conductivity (K_s), volumetric moisture at saturation (θ_s), and capillary length (h_g) for the surfaces in Parque da Jaqueira.

Table 3 - Parameters of the shape of the retention curve and hydraulic properties of the superficial soils of the CU, CR, and UPG.

Area / Sample	n	m	η	c_p	S ($mm.s^{-0,5}$)	K_s ($mm.h^{-1}$)	θ_s ($cm^3.cm^{-3}$)	h_g (mm)	Hydrological Classification
CU 1	**2.45**	**0.18**	**7.44**	**1.95**	**0.13**	**4.07**	**0.40**	**-22.66**	**B**
CU 2	**2.30**	**0.13**	**9.78**	**2.15**	**0.42**	**29.32**	**0.40**	**-29.86**	**A**
CU 3	**2.24**	**0.11**	**11.37**	**2.25**	**0.30**	**9.76**	**0.50**	**-34.19**	**A**
CU 4	**2.31**	**0.13**	**9.56**	**2.13**	**0.30**	**9.61**	**0.41**	**-39.29**	**A**
CU 5	**2.37**	**0.16**	**8.37**	**2.04**	**0.23**	**8.21**	**0.38**	**-31.69**	**A**
CU 6	**2.37**	**0.16**	**8.39**	**2.04**	**0.14**	**10.76**	**0.40**	**-8.54**	**A**
CU 7	**2.35**	**0.15**	**8.79**	**2.07**	**0.22**	**7.67**	**0.37**	**-32.93**	**A**
CU 8	**2.22**	**0.10**	**12.05**	**2.28**	**0.13**	**102.42**	**0.51**	**-0.52**	**A**
Mean	**2.33**	**0.14**	**9.47**	**2.11**	**0.23**	**22.73**	**0.42**	**-24.96**	**A**
SD	**0.08**	**0.03**	**1.58**	**0.11**	**0.10**	**33.09**	**0.05**	**13.60**	**-**
CV	**0.03**	**0.20**	**0.17**	**0.05**	**0.44**	**1.46**	**0.13**	**0.55**	**-**
CR 1	**2.46**	**0.19**	**7.38**	**1.95**	**0.66**	**256.86**	**0.42**	**-7.61**	**A**
CR 2	**2.29**	**0.13**	**10.02**	**2.16**	**0.31**	**25.38**	**0.40**	**-16.83**	**A**
CR 3	**2.51**	**0.20**	**6.96**	**1.91**	**0.70**	**62.89**	**0.37**	**-39.92**	**A**
CR 4	**2.49**	**0.20**	**7.08**	**1.92**	**0.48**	**44.24**	**0.36**	**-27.81**	**A**
CR 5	**2.35**	**0.15**	**8.69**	**2.06**	**0.31**	**10.96**	**0.35**	**-23.55**	**A**
CR 6	**2.57**	**0.22**	**6.50**	**1.86**	**0.82**	**72.40**	**0.36**	**-51.57**	**A**
CR 7	**2.56**	**0.22**	**6.57**	**1.87**	**0.98**	**69.88**	**0.35**	**-75.95**	**A**
CR 8	**2.46**	**0.19**	**7.35**	**1.95**	**0.59**	**45.04**	**0.37**	**-40.87**	**A**
Mean	**2.46**	**0.19**	**7.57**	**1.96**	**0.61**	**73.46**	**0.42**	**-35.51**	**A**
SD	**0.10**	**0.03**	**1.20**	**0.10**	**0.23**	**77.13**	**0.13**	**21.62**	**-**
CV	**0.04**	**0.18**	**0.16**	**0.05**	**0.39**	**1.05**	**0.31**	**0.61**	**-**
UPG 1	**2.35**	**0.15**	**8.71**	**2.07**	**0.17**	**100.48**	**0.54**	**-1.09**	**A**
UPG 2	**2.38**	**0.16**	**8.23**	**2.03**	**0.34**	**306.65**	**0.54**	**-1.34**	**A**
UPG 3	**2.37**	**0.15**	**8.49**	**2.05**	**0.30**	**179.89**	**0.54**	**-1.70**	**A**
UPG 4	**2.33**	**0.14**	**9.06**	**2.09**	**0.33**	**79.81**	**0.48**	**-5.83**	**A**
UPG 5	**2.35**	**0.15**	**8.65**	**2.06**	**0.33**	**152.46**	**0.53**	**-2.92**	**A**
UPG 6	**2.26**	**0.12**	**10.61**	**2.20**	**0.31**	**25.88**	**0.47**	**-15.20**	**A**
UPG 7	**2.31**	**0.14**	**9.43**	**2.12**	**0.66**	**227.52**	**0.46**	**-8.14**	**A**
UPG 8	**2.32**	**0.14**	**9.28**	**2.11**	**0.53**	**542.20**	**0.49**	**-2.30**	**A**
Mean	**2.33**	**0.14**	**9.06**	**2.09**	**0.37**	**201.86**	**0.51**	**-4.81**	**A**
SD	**0.04**	**0.01**	**0.75**	**0.05**	**0.15**	**163.24**	**0.03**	**4.86**	**-**
CV	**0.02**	**0.10**	**0.08**	**0.02**	**0.41**	**0.81**	**0.07**	**1.01**	**-**
SD = Standart Deviation					**CV = Coefficient of Variation**				

Source: Authors (2019).

The values of the shape parameter n shown in Table 2 are in accordance with the values obtained by Furtunato et al. (2013). However, the shape parameter η, presented in general, lower values than those obtained by the mentioned study.

According to Table 2, 87.50% of CU soils (2, 3, 4, 5, 6, 7, and 8), and 50% of UPG soils (1, 4, 6, and 8) are classified as sandy clay loam. For this textural class, the shape parameters of the retention curve ranged from 2.22 to 2.37 for n, and from 8.37 to 12.05 for η. Souza et al. (2008) determined for this same textural class values of n and η equal to 2.12 and 20.23, respectively.

The shape factor n for the children's recreation area classified as loamy sand (1, 3, 4, 5, 6, 7, and 8) varied between 2.35 and 2.57, while η ranged between 6.50 and 8.69. These values are consistent with those observed by Souza et al. (2008), who obtained values of 2.31 and 9.54 for n and η, respectively. The results are also in agreement with the study developed by Santos et al. (2012), which detected n of 2.57 and η of 6.62.

The sandy loam textural class embraces 12.50% of CR and 50% of UPG soils. For them, the shape parameters n and η ranged from 2.29 to 2.38 and 8.23 to 10.02, respectively. These numbers are in concordance with those verified by Souza et al. (2008). However, they diverge from those obtained by Santos et al. (2012), who found values of 2.19 for n and 1.34 for η.

The shape parameters depend in general on the type of soil. The values of the parameters n and m for coarser soils (predominantly sandy soils) usually are high. Globally, the values presented in this work were more elevated in soils with higher sand content, and inversely, the values of η and c_p were lower for the same points.

Sorptivity is a hydrodynamic parameter that depends on the initial soil moisture conditions. The variability observed in all tested points is directly related to the initial soil moisture at the moment that the test is performed.

One can observe that the sorptivity showed a minimum value of 0.13 $mm.s^{-0.5}$ and a maximum of 0.98 $mm.s^{-0.5}$. Alagna et al. (2016) analyzing a soil classified as sandstone, detected sorptivity ranging from 0.90 to 3.03 $mm.s^{-0.5}$ for a depth of 3 cm, and from 0.66 to 0.87 $mm.s^{-0.5}$ for a depth of 1.50 m. Oliveira Júnior et al. (2014) observed mean values of sorptivity of 0.79 and 0.93 $mm.s^{-0.5}$ for pasture and caatinga areas, respectively.

The texture did not present a direct correlation with the saturated hydraulic conductivity (K_s). This outcome followed the performance of Rahmati et al. (2018) analyzes for more than 3000 infiltration curves around the world. The sandy loam soils showed significant variability of Ks, with values ranging between 25.38 and 306.65 $mm.h^{-1}$. Aiello et al. (2014) determined a lower variability for this textural class, obtaining values between 8.28 and 46.80 $mm.h^{-1}$. Alagna et al. (2016) established values between 36.60 and 958.10 $mm.h^{-1}$ for depths of 3 cm, and between 3.2 and 45 $mm.h^{-1}$ for depths of 1.50m. Bagarelo et al. (2014) found values ranging from 20.1 to 488 $mm.h^{-1}$.

The coefficient of saturated hydraulic conductivity for sandy clay loam soils ranged from 7.67 to 542.2 $mm.h^{-1}$. The magnitude of the K_s obtained by Souza et al. (2008) was 180 $mm.h^{-1,}$ with a field density fluctuating between 1.12 and 1.22 $g.cm^{-3}$. Di Prima et al. (2016) obtained a saturated hydraulic conductivity of 12.96 $mm.h^{-1}$ with a field density of 1,191 $g.cm^{-3}$. According to Coutinho et al. (2016), these differences result from the dependence of the hydrodynamic properties in other parameters besides the textural properties. In fact, the structure of the soils interferes with the distribution and connection of the pores, influencing the hydrodynamic properties.

The loamy sand textural class showed a minimum K_s value of 4.07 $mm.h^{-1}$ and a maximum of 256.86 $mm.h^{-1}$. Santos et al. (2012) determined for this texture, an average value of 262.8 $mm.h^{-1}$, while Souza et al. (2008) obtained a hydraulic conductivity of 108 $mm.h^{-1}$.

The further analysis of Table 3 reports that only one sample obtained hydrological classification in group B (CU1). The others were classified in group A, with high hydraulic conductivity. In addition, it is important to mention the values presented in the UPG tests, which were much higher than those observed in CU and CR. Although 87.50% of CU soils are in group A, some values have approached the classification limits of group B, i.e., CU7 and CU5.

These analyzes demonstrate that, despite the soils having the same grain size distribution (sandy clay loam) and hydrological (group A) classifications, the values of hydraulic conductivity can present a high variability. This proves that the cover type and surface soil use have a direct influence on the performance of the hydraulic properties of the soil.

Figure 4 shows average retention curves, θ (h), and hydraulic conductivity, K (θ), for the three analyzed areas. The difference between the retention curves is minimal. However, one can note greater water retention by the UPG from the 10 cm potential. On the other hand, CR was the area with the lowest retention capacity for moisture below 0.1 $cm^3.cm^{-3}$. In addition, UPG has water storage slightly higher than CR and CU.

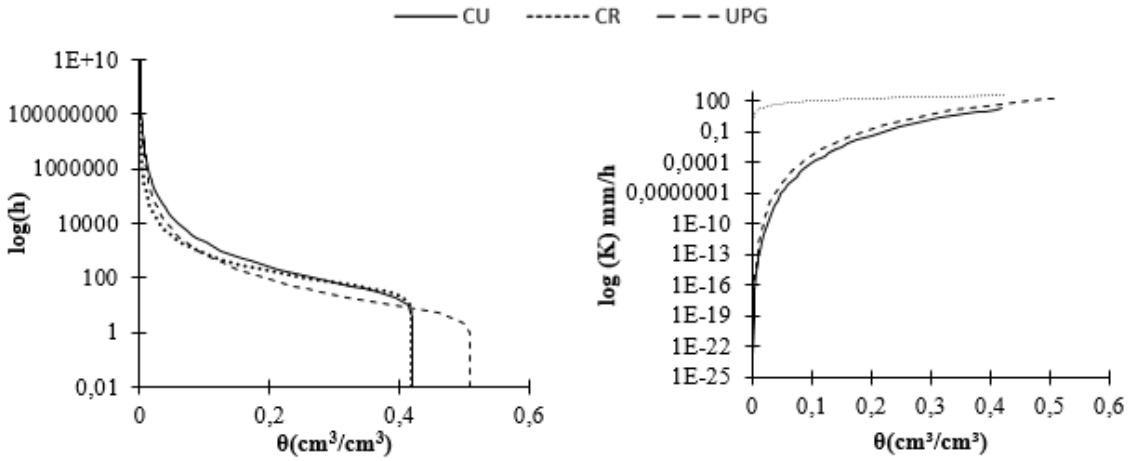

Figure 4 – Average curves of retention and hydraulic conductivity, respectively, of the superficial soils of the CU, CR and UPG.
Source: Authors (2019).

Regarding the water conduction capacity (K(θ)), CR reflects a better hydraulic conductivity than the other surfaces. However, one can expect, due to the behavior of the curves, a trend of higher driving capacity in UPG for values greater than 0.4 $cm^3.cm^{-3}$.

Figure 5 shows the adjustments made from Burdine to Mualem, which are sound for the three areas. The adjusted retention curves reflect good representativeness to the Burdine model for values close to saturation and values with lower moisture.

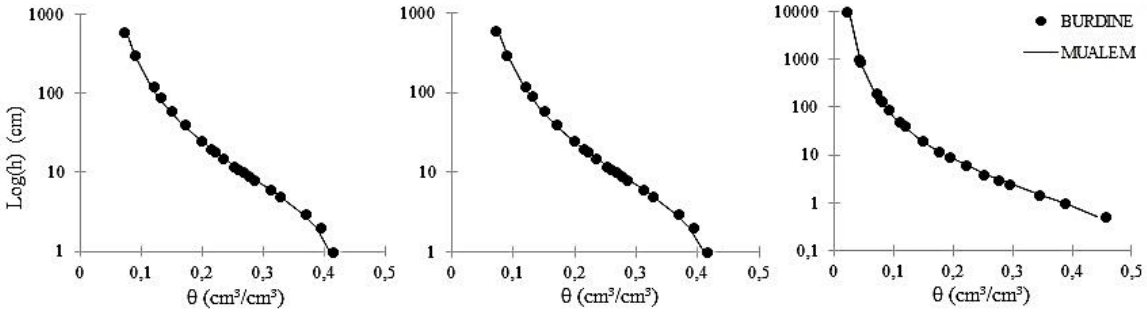

Figure 5 – Adjustment of Burdine's model for the Mualem's hypothesis for the CU, CR and UPG, respectively.
Source: Authors (2019).

After the adjustments, the simulation of the flow variables (cumulative runoff, cumulative evaporation, cumulative infiltration, and water storage) was estimated using Hydrus 1D. Figure 6 shows the characteristic curves of each variable in the three analyzed areas.

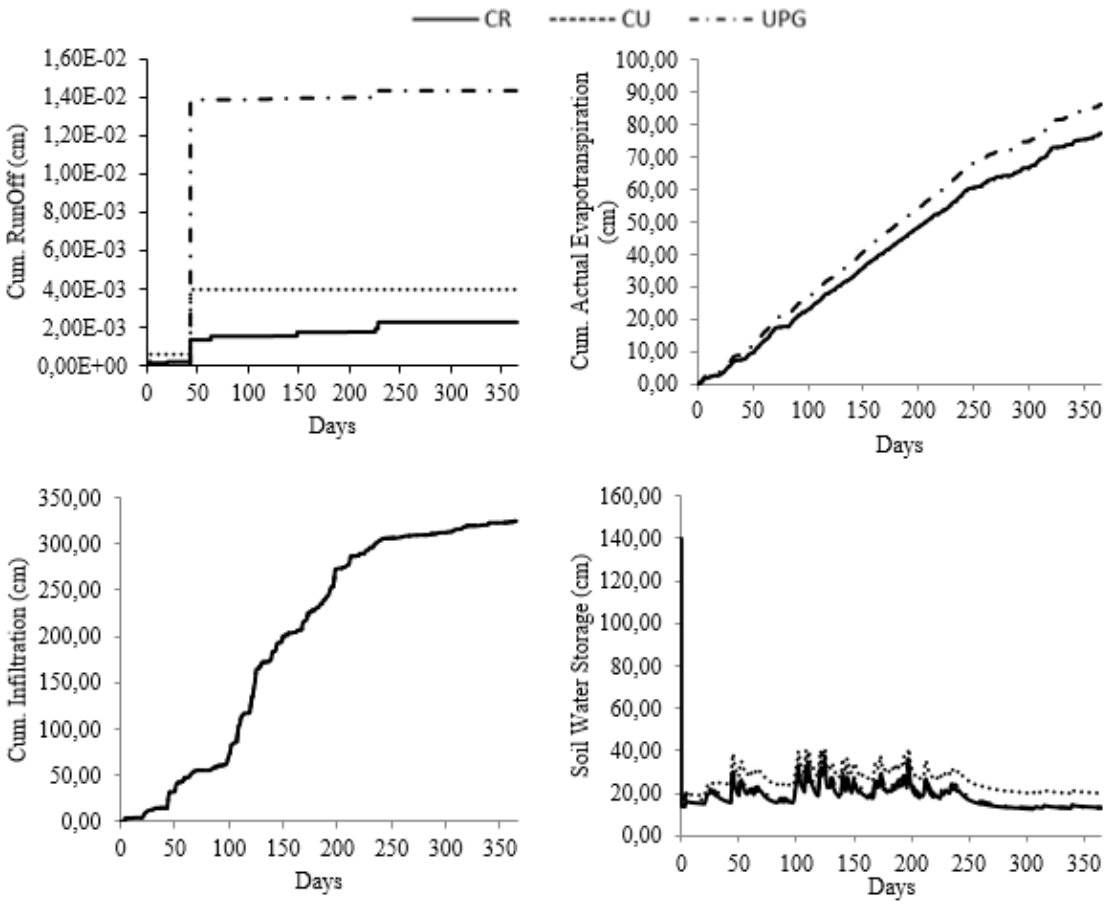

Figure 6 – Hydrus' outputs of the Cumulative Runoff; Cumulative actual Evapotranspiration; Cumulative Infiltration; and Soil Water Storage.
Source: Authors (2019).

The surface runoff was more significant for urban park gardens, followed by the community use area and children's recreation area. Despite these differences, the order of magnitude of the runoff demonstrates that its generation capacity is low.

One can observe that there is no difference between the cumulative infiltration rates because the entire daily precipitation is less than the infiltration capacity of the soil. In this way, for the children's recreation area, from the 325 cm annually precipitated, 23.78% was converted into real evaporation. But most of this total precipitation (more than 70%) is converted into drainage at the base of the profile, which will allow the groundwater recharge.

Regarding the urban park gardens, the real evaporation corresponds to 26.52% of the total precipitated, with drainage at the base of the profile, slightly less than that of the children's recreation area. Although the urban park gardens and the children's recreation area have different types of use, due to their textural compositions being sandy clay loam, the hydrological behaviors of the two surfaces were similar.

CONCLUSIONS

This study demonstrated the capacity of urban parks to contribute to the management of urban rainwater. This happens especially concerning the rescue and/or enhancement of processes of the hydrological cycle, mainly infiltration and evapotranspiration.

Despite the diverse use existing in Parque da Jaqueira, the analyzed areas (community use, children's recreation and gardens), showed sound water infiltration capacities in the soil. Regarding the hydraulic conductivity, 23 samples were hydrologically classified in group A, which presents good conditions for water conduction in the soil. Besides that, comparing the three areas, the gardens of high parks showed greater values of hydraulic conductivity. This result reflected in shorter times of water infiltration in the soil.

The hydrodynamic characterization was based on the Beerkan Methodology, while Hydrus' model was used for the simulation of soil water transfer processes. These two tools made it possible to obtain hydrodynamic reference parameters on three soils of different surface use. These results and discussions help to understand the behavior of the components of water balance in an urban park, becoming a reference for possible studies.

ACKNOWLEDGMENTS

This work was carried out with the support of the project "Transfer of Water and Mixtures of Reactive Pollutants in Anthropized Soils" (CNPq process No. 436875/2018-7).

REFERENCES

Aiello, R., Bagarello, S., Consoli, S., Di Prima, S., Giordano, G., & Lovino, M. (2014). An assessment of the Beerkan method for determining the hydraulic properties of a Sandy loam soil. *Geoderma*, *235–236*, 300-307.

Alagna, V., Bagarello, V., Di Prima, S., Giordano, G., & Iovino, M. (2016). Testing infiltration run effects on the estimated water transmission properties of a sandy-loam soil. *Geoderma*, *267*, 24-33.

Alcântara, L. R. P., Martins, L. A., Aguiar Costa, I. R., Oliveira Barros, V. H., Santos Neto, S. M., Coutinho, A. P., & Antonino, A. C. D. (2019). Avaliação de modelos probabilísticos para chuvas intensas nas mesorregiões do estado de Pernambuco (Evaluation of probabilistic models for heavy rains in the mesoregions of the state of Pernambuco). *Journal of Environmental Analysis and Progress*, *4*(1), 90-103.

Angulo-Jaramillo, R., Bagarello, V., Di Prima, S., Gosset, A., Iovino, M., & Lassabatere, L. (2019). Beerkan Estimation of Soil Transfer parameters (BEST) across soils and scales. *Journal of Hydrology (Amsterdam)*, *576*, 239-261.

Anguluri, R., & Narayanan, P. (2017). Role of green space in urban planning: outlook towards smart cities. *Urban Forestry & Urban Greening*, (25), 58-65.

Associação Brasileira de Normas Técnicas – ABNT. (1984). *NBR 7181: análise granulométrica (granulometric analysis)*. Rio de Janeiro: ABNT.

Bagarelo, V., Di Prima, S., & Lovino, M. (2014). A test of the Beerkan Estimation of Soil Transfer parameters (BEST) procedure. *Geoderma*, *221-222*, 20-27.

Berland, A., Shiflett, S. A., Shuster, W. D., Garmestani, A. S., Goddard, H. C., Herrmann, D. L., & Hopton, M. E. (2017). The role of trees in urban stormwater management. *Landscape and Urban Planning*, *162*, 167-177.

Brooks, R. H., & Corey, A. T. (1964). *Hydraulic properties of porous media* (No. 3, Hydrology Paper, 27 p.). Fort Collins: Colorado State University.

Burdine, N. T. (1953). Realtive permeability calculations from pore-sized distribution data. *American Institute Mining and Metallurgy Engineering*, *198*, 71-77.

Cerdà, A., Keesstra, S., Burguet, M., Pereira, P., Lucasborja, M. E., & Martinez, M. J. F. (2016). Seasonal changes of the infiltration rates in urban parks of Valencia City, Eastern Spain. In *Proceedings of the Geophysical Research Abstracts. EGU General Assembly Conference* (pp. 18110).

Conway, T. M., Shakeel, T., & Atallah, J. (2011). Community groups and urban forestry activity: drivers of uneven canopy cover? *Landscape and Urban Planning*, *101*(4), 321-329.

Coutinho, A. P., Lassabatere, L., Montenegro, S., Antonino, A. C. D., Angulo-Jaramillo, R., & Cabral, J. J. (2016). Hydraulic characterization and hydrological behaviour of a pilot permeable pavement in an urban centre, Brazil. *Hydrological Processes*, *30*, 4242-4254.

de Condappa, D., Soria Ugalde, J. M., Angulo-Jaramillo, R., & Haverkamp, R. (2002). *Méthode Beerkan. Caractérisation des propriétés hydrodynamiques des sols non saturés. Rapport interne Hydrologie de la Zone Non Saturés – LTHE* (82 p). Grenoble: Université de Grenoble.

Deutscher, J., Kupec, P., Kučera, A., Urban, J., Ledesma, J. L., & Futter, M. (2019). Ecohydrological consequences of tree removal in an urban park evaluated using open data, free software and a minimalist measuring campaign. *The Science of the Total Environment*, *655*, 1495-1504.

Di Prima, S., Lassabatere, L., Bagarello, V., Lovino, M., & Ângulo-Jaramillo, R. (2016). Testing a new automated single ring infiltrometer for Beerkan infiltration experiments. *Geoderma*, *262*, 20-34.

Empresa Brasileira de Pesquisa Agropecuária – EMBRAPA, & Centro Nacional de Pesquisa de Solos (1997). *Manual de Métodos de Análise de Solo* (2. ed.). Rio de Janeiro, RJ: EMBRAPA.

Ferreira, L. I. E. P. (2007). Parque Urbano (Urban Park). *Paisagem Ambiente: Ensaios*, *23*, 20-33.

Furtunato, O. M., Montenegro, S. M. G. L., Antonino, A. C. D., Oliveira, L. M. M., Souza, E. S., & Moura, A. E. S. S. (2013). Variabilidade espacial de atributos físico-hídricos de solos em uma bacia experimental no estado de Pernambuco (Spatial Variability of Physical and Hydraulic Attributes of Soils in an Experimental Basin in the State of Pernambuco). *Revista Brasileira de Recursos Hídricos*, *18*, 135-147.

Gomes, M. A. S. (2014). Parques urbanos, políticas públicas e sustentabilidade (Urban Parks, Public Policies, and Sustainability). *Mercator (Fortaleza)*, *13*(2), 79-90.

Gonzalez-Sosa, E., Braud, I., Piña, R. B., Loza, C. A. M., Salinas, N. M. R., & Chavez, C. V. (2017). A methodology to quantify ecohydrological services of street trees. *Ecohydrology & Hydrobiology*, *17*(3), 190-206.

Haverkamp, R., & Parlange, J. Y. (1986). Predicting the water retention curve from particle size distribution: I Sandy soils without organic matter. *Soil Science*, *142*, 325-335.

Haverkamp, R., Parlange, J. Y., Cuenca, R., Ross, P. J., & Steenhuis, T. S. (1998). Scaling of the Richards equation and its application to watershed modeling. In G. Sposito (Ed.), *Scale dependence and scale invariance in hydrology* (p. 190-223). Cambridge: Cambridge University Press.

Haverkamp, R., Ross, P. J., Smettem, K. R. J., & Parlange, J. Y. (1994). Three dimensional analysis of infiltration from the disc infiltrometer: 2. Physically based infiltration equation. *Water Resources Research*, *30*, 2931-2935.

Lassabatère, L., Angulo-Jaramillo, R., Soria, J. M., Cuenca, R., Braud, I., & Haverkamp, R. (2006). Beerkan estimation of soil transfer parameters through infiltration experiments – BEST. *Soil Science Society of America Journal*, *70*, 521-532.

Macedo, M. B., Lago, C. A. F., & Mendiondo, E. M. (2019). Stormwater volume reduction and water quality improvement by bioretention: potentials and challenges for water security in a subtropical catchment. *The Science of the Total Environment*, *647*, 923-931.

Marquardt, D. W. (1963). An algorithm for least squares estimation of non linear parameters. *SIAM Journal on Applied Mathematics*, *11*, 431-441.

Melo, T. A. T., Coutinho, A. P., Cabral, J. J. D. S. P., Antonino, A. C. D., & Cirilo, J. A. (2014). Jardim de chuva: sistema de biorretenção para o manejo das águas pluviais urbanas (Rain garden: bioretention system for urban stormwater management). *Ambiente Construído*, *14*(4), 147-165.

Millward, A. A., Paudel, K., & Briggs, S. E. (2011). Naturalization as a strategy for improving soil physical characteristics in a forested urban park. *Urban Ecosystems*, *14*(2), 261-278.

Mualem, Y. A. (1976). A new model for predicting the hydraulic conductivity of unsatured porous media. *Water Resources Research*, *12*, 513-522.

Oliveira Júnior, J. A. S., Souza, E. S., Correa, M. M., Lima, J. R. S., Souza, R. M. S., & Silva Filho, L. A. (2014). Variabilidade espacial de propriedades hidrodinâmicas de um Neossolo Regolítico sob pastagem e caatinga (Spatial variability of hydrodynamic properties of a Regolithic Neosoil under pasture and 'caatinga'). *Revista Brasileira de Engenharia Agrícola e Ambiental*, *18*, 631-639.

Pedron, F. A., & Dalmolin, R. S. D., Azevedo, A. C., & Ksminski, J. (2004). Solos urbanos (Urban Soils). *Ciência Rural*, *34*(5), 1647-1653.

Phillips, T. H., Baker, M. E., Lautar, K., Yesilonis, I., & Pavao-Zuckerman, M. A. (2019). The capacity of urban forest patches to infiltrate stormwater is influenced by soil physical properties and soil moisture. *Journal of Environmental Management*, *246*, 11-18.

Rahmati, M., Weihermüller, L., Vanderborght, J., Pachepsky, Y. A., Mao, L., Sadeghi, S. H., Moosavi, N., Kheirfam, H., Montzka, C., Van Looy, K., Toth, B., Hazbavi, Z., Al Yamani, W., Albalasmeh, A. A., Alghzawi, M. Z., Angulo-Jaramillo, R., Antonino, A. C. D., Arampatzis, G., Armindo, R. A., Asadi, H., Bamutaze, Y., Batlle-Aguilar, J., Béchet, B., Becker, F., Blöschl, G., Bohne, K., Braud, I., Castellano, C., Cerdà, A., Chalhoub, M., Cichota, R., Císlerová, M., Clothier, B., Coquet, Y., Cornelis, W., Corradini, C., Coutinho, A. P., de Oliveira, M. B., de Macedo, J. R., Durães, M. F., Emami, H., Eskandari, I., Farajnia, A., Flammini, A., Fodor, N., Gharaibeh, M., Ghavimipanah, M. H., Ghezzehei, T. A., Giertz, S., Hatzigiannakis, E. G., Horn, R., Jiménez, J. J., Jacques, D., Keesstra, S. D., Kelishadi, H., Kiani-Harchegani, M., Kouselou, M., Kumar Jha, M., Lassabatere, L., Li, X., Liebig, M. A., Lichner, L., López, M. V., Machiwal, D., Mallants, D., Mallmann, M. S., de Oliveira Marques, J. D., Marshall, M. R., Mertens, J., Meunier, F., Mohammadi, M. H., Mohanty, B. P., Pulido-Moncada, M., Montenegro, S., Morbidelli, R., Moret-Fernández, D., Moosavi, A. A., Mosaddeghi, M. R., Mousavi, S. B., Mozaffari, H., Nabiollahi, K., Neyshabouri, M. R., Ottoni, M. V., Ottoni Filho, T. B., Pahlavan-Rad, M. R., Panagopoulos, A., Peth, S., Peyneau, P.-E., Picciafuoco, T., Poesen, J., Pulido, M., Reinert, D. J., Reinsch, S., Rezaei, M., Roberts, F. P., Robinson, D., Rodrigo-Comino, J., Rotunno Filho, O. C., Saito, T., Suganuma, H., Saltalippi, C., Sándor, R.,

Schütt, B., Seeger, M., Sepehrnia, N., Sharifi Moghaddam, E., Shukla, M., Shutaro, S., Sorando, R., Stanley, A. A., Strauss, P., Su, Z., Taghizadeh-Mehrjardi, R., Taguas, E., Teixeira, W. G., Vaezi, A. R., Vafakhah, M., Vogel, T., Vogeler, I., Votrubova, J., Werner, S., Winarski, T., Yilmaz, D., Young, M. H., Zacharias, S., Zeng, Y., Zhao, Y., Zhao, H., & Vereecken, H. (2018). Development and analysis of the Soil Water Infiltration Global database. *Earth System Science Data*, *10*(3), 1237-1263. http://dx.doi.org/10.5194/essd-10-1237-2018

Rawls, W. J., Ahuja, L. R., Brakensiek, D. L., & Shirmohammadi, A. (1993). Infiltration and soil water movement. handbook of hydrology. In R. David (Ed.), *Maidment* (pp. 5.1-5.51). USA: Mc-Graw-Hill, Inc.

Richards, L. A. (1931). Conduction liquids in porous medium. *Physics*, *1*, 318-333.

Sakata, F. G., & Gonçalves, F. M. (2019). Um novo conceito para parque urbano no Brasil do século XXI. *Paisagem e Ambiente (a new concept for urban park in brazil on the 21st century)*, *30*(3), 1-21.

Santos, C. A. G., Silva, J. F. C. B. C., & Silva, R. M. (2012). Caracterização hidrodinâmica dos solos da bacia experimental do Riacho Guaraíra utilizando o Método Beerkan (Hydrodynamic Characterization of the Soils in the Guaraíra River Experimental Basin Using the Beerkan Method). *Revista Brasileira de Recursos Hídricos*, *17*, 149-160.

Santos, P. T. S., Santos, S. M., Montenegro, S. M. G. L., Coutinho, A. P., Moura, G. S. S., & Antonino, A. C. D. (2013). Telhado verde: desempenho do sistema construtivo na redução do escoamento superficial (Green roof: performance of the constructive system in the reduction of runoff). *Ambiente Construído*, *13*(1), 161-174.

Šimůnekm, J., van Genuchten, M. Th., & Šejna, M. (2008). Development and applications of the HYDRUS and STANMOD software packages and related codes. *Vadose Zone Journal*, *7*(2), 587-600.

Souza, E. S., Antonino, A. C. D., Ângulo-Jaramillo, R., & Netto, A. M. (2008). Caracterização hidrodinâmica de solos: aplicação do método Beerkan (Hydrodynamic characterization of soils: application of the Beerkan method). *Revista Brasileira de Engenharia Agrícola e Ambiental*, *12*, 128-135.

van Genuchten, M. T. H. (1980). A closed-form equation for predicting the hydraulic conductivity of unsaturated soils. *Soil Science Society of America Journal*, *44*, 892-898.

Author contributions:

Artur Paiva Coutinho: Conceptualization; Methodology; Software; Validation; Formal analysis; Investigation; Project administration; Data curation; Writing – original draft; Visualization; Funding acquisition.

Edilson Gomes de França: Conceptualization; Methodology; Software; Writing – review and editing.

Alfredo Ribeiro Neto: Software; Validation; Resources; Writing – review and editing; Supervision.

Tássia dos Anjos Tenório de Melo: Conceptualization; Methodology; Validation; Writing – review and editing.

Severino Martins dos Santos Neto: Conceptualization; Investigation; Methodology; Writing – review and editing; Writing – original draft.

Vitor Hugo de Oliveira Barros: Investigation; Resources; Writing – review and editing; Writing – original draft.

Lucas Ravellys Pyrrho de Alcântara: Investigation; Data curation; Writing – review and editing.

Antonio Celso Dantas Antonino: Writing – review and editing; Supervision; Project administration; Funding acquisition.